

Reducing Tannery Wastewater Pollutants through a Magnetic-Field and Ozone-Treatment Electrocoagulation System using Response Surface Methodology

Edwar Aguilar Ascon^{1*}, Liliana Marrufo Saldaña², Walter Neyra Ascón³

¹ Instituto de Investigación Científica (IDIC), Universidad de Lima, Av. Javier Prado Este 4600, Surco, Lima, Perú

² Centro de Innovación Productiva y Transferencia Tecnológica del Cuero, Calzado e Industrias Conexas (CITEccal Lima)-ITP, Av. Caquetá 1300, Rímac, Lima, Peru

³ Universidad de Lima, Av. Javier Prado Este 4600, Surco, Lima, Perú

* Corresponding author's e-mail: eaguilaa@ulima.edu.pe

ABSTRACT

This study assessed the effectiveness of integrating electrocoagulation, magnetic fields, and ozonation technologies to remove chemical oxygen demand (COD) and total suspended solids (TSS) from tannery wastewater. Furthermore, the effects of their key operating factors were determined. To achieve this goal, an electrocoagulation reactor coupled with a magnetic-field generator was used and the response surface methodology was applied through a Box-Behnken experimental design. Here, current intensity (I), treatment time (T), and ozone concentration (O₃) are considered the influencing factors. Likewise, the removal percentages of COD and TSS serve as response indicators. The results indicate that T, I, and O₃ are significant for the removal of COD and TSS at a confidence level of p-value < 0.05. For COD, the optimal operating conditions are I = 6.8 A, T = 30 min, and O₃ = 10 mg/l; and for TSS, the optimal conditions are I = 5.72 A, T = 28 min, and O₃ = 7.8 mg/l. These conditions yield removal efficiencies of 41.8% for COD and 97.9% for TSS. The findings suggest that integrating these technologies is a viable alternative for mitigating the pollution issues caused by the tannery industry.

Keywords: tannery wastewater, COD, TSS, electrocoagulation, aluminum electrodes, ozone, response surface.

INTRODUCTION

The leather, footwear, and related supply chain make a significant contribution to employment rates. In Peru, this industry is disseminated across three regions: Lima, Arequipa, and Trujillo. Despite the continuous influx of substantial volumes of imported footwear for over two decades, resulting in decreased production levels, numerous micro, small, and even some large tanneries still continue to produce leather. The survival of companies within this industry is related to their ability to attain certain levels of productivity and competitiveness. Nevertheless, there are critical and constraining factors that require attention, notably regarding the handling of their effluents and solid waste, which are characterized by elevated levels of pollutants. Although the country's

environmental regulations have established benchmarks for these effluents, their effective enforcement has been impeded by the intricate nature of production processes that involve diverse chemical substances discharged as residues into the effluents. Subsequently, these residues are stored and managed as blends. Among the primary pollutants generated, one can identify biochemical oxygen demand (BOD), chemical oxygen demand (COD), total suspended solids (TSS), sulfides, ammonia, chlorides, and those originating from the tanning agents employed. A notable example among these agents is basic chromium sulfate, a globally employed tanning agent due to the physical and mechanical attributes it provides to leather. Consequently, the presence of chromium in effluents has prompted numerous studies to explore alternative removal methods for this pollutant.

Electrocoagulation has demonstrated efficiency in removing contaminants, including COD, BOD, TSS, and heavy metals, such as chromium (Kanagaraj et al., 2014; De la Luz-Pedro et al., 2019; Aguilar et al., 2019; Liu et al., 2018). Nevertheless, there is evidence indicating that its combination with a magnetic field (Ghernaout et al., 2009; Ibanez et al., 2012) or advanced ozone-based oxidation (Barzegar et al., 2019; Bilińska et al., 2019) amplifies its efficiency, even resulting in reduced energy consumption (Liu et al., 2018). Several studies have assessed the combination of at least two of the processes described in this study (electrocoagulation (EC), magnetic field, and ozonation) for the treatment of tannery wastewater as well as different types of effluents. One of these studies was published by Ibanez et al. (2012), wherein a combined electrochemical-magnetic approach was employed to demonstrate that the presence of a magnetic field enhances the precipitation of suspended coagulants, resulting in a 30% increase in turbidity removal. In addition, Irki et al. (2017) applied a magnetic field to enhance the electrocoagulation process for decolorizing methyl orange. Through their experimental work, they observed that the removal of methyl orange increased from 74%, reported using only electrocoagulation to 95% after the magnetic field was introduced. Likewise, Hernández-Ortega et al. (2010) reported that coupling EC with ozone proves effective as a comprehensive treatment for discharging industrial effluents into municipal sewers. They achieved over 90% and 60% reduction in the color as well as turbidity of wastewater and COD, respectively. Furthermore, Asaithambi et al. (2016) documented 100% and 95% efficiencies in color and COD removal, respectively. They concluded that the hybrid EC process could be successfully applied to remove pollutants from effluents.

Electrocoagulation is commonly used for purifying wastewater. Metal cations are electrochemically dissolved locally through physical and chemical processes using an oxidized sacrificial anode (a metal electrode) (Ebba, 2021). This anode dissolves to generate coagulant species that destabilize colloidal particles, forming flocs that, through a flotation process, rise to the surface, while another portion precipitates (Esfandyari et al., 2019; Aguilar et al., 2020). Iron and aluminum electrodes are the prevailing choices in EC due to their availability, non-toxicity, and established reliability (Moussa et al., 2017). Metal cations like Al^{3+} and Fe^{2+} are produced at the anode and thus

do not need to be externally supplied. Concurrently, hydrogen gases are generated at the cathode, inducing the flotation of contaminants (Holt et al., 2005). Recent research indicates that electrocoagulation is environmentally friendly and exhibits high efficiency in contaminant removal (Nugroho et al., 2019). Likewise, it eliminates the need for chemical products (Koyuncu and Ariman, 2020), and the volume of sludge produced is reduced, compared with that generated through chemical treatment (Papadopoulos et al., 2019). According to Dermentzis (2016), the anodic and cathodic reactions that occur in aluminum and iron electrodes are the following:

Anodic reaction for aluminum:



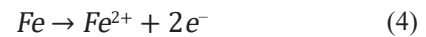
Cathodic reaction for aluminum:



General reaction:



Anodic reaction for iron:



Cathodic reaction for iron:



The use of magnetic technology holds promise as a wastewater treatment method: it enhances the separation of suspended particles (Johanet et al., 2004) and impacts the physicochemical properties of water, including light absorbance, pH, and surface tension (Cho and Lee, 2005). The magnetic field has the capacity to modify the spin states of reactants and intermediates, influencing the structure of the formed molecules and the adsorption of intermediates on the electrode surface. As a result, it can change the kinetics and selectivity of electrochemical reactions (Yasri et al., 2022; Garcés-Pineda et al., 2019). Furthermore, the magnetic field effect enhances the activity of chemicals and coagulation, facilitating the contact of suspended solids in water with the flocculant and thereby increasing the flocculation rate (Guo et al., 2014).

Ozone (O_3), known for its robust oxidation capabilities, is extensively used in water disinfection and the degradation of organic contaminants (Liu et al., 2021). In addition, advanced oxidation processes based on ozone are effective and straightforward methods for treating refractory contaminants in wastewater without generating secondary waste (Joseph et al., 2021). An inherent property of ozone is its water solubility, which is 13 times

greater than that of oxygen. This characteristic has led to its widespread application in the degradation of several organic compounds (Malik et al., 2020).

Given the challenges posed by the tannery industry and leveraging current knowledge, this study aimed to assess the effectiveness of removing COD and TSS from tannery wastewater. This objective was pursued through the integration of electrocoagulation, magnetic field, and ozonation technologies, employing a response surface methodology.

MATERIALS AND METHODS

Characteristics of tannery wastewater

The tannery wastewater was collected from the tanning and effluent treatment processes at the Leather and Footwear Technological Innovation Center and Related Industries (CITEccal). Table 1 presents a subset of its monitored parameters, revealing elevated conductivity values attributed to the salts used in the tanning processes, as well as high concentrations of COD and TSS.

Electrocoagulation, magnetic field, and ozonation reactor

The testing reactor was designed in a batch configuration, measuring 16 cm in length, 16 cm in width, and 22 cm in height (Figure 1). Eight aluminum electrodes, each measuring 10 cm in width, 10 cm in length, and with an area of 100 cm², were strategically placed to serve as both

Table 1. Physicochemical effluent analysis

Parameter	Value
Total suspended solids (mg/l)	1050
Chemical oxygen demand COD (mg/l)	3815
Biochemical oxygen demand BOD (mg/l)	823
Turbidity (mg/l)	1200
Total chromium	50.24
Chromium IV	<0.005
Oils and Fats (mg/l)	39.8
pH	7.28
Conductivity (μS/cm)	16200
Fecal coliforms (MPN/100 ml)	4.5
Sulfurs (mg/l)	70.9
Ammonia nitrogen (mg/l)	445

anodes and cathodes. To mitigate the high conductivity of the effluent, a series arrangement of electrodes was adopted, maintaining a 2 cm gap between the electrodes to reduce the electrical current demand. A copper coil attached to the reactor generated the magnetic field, which was powered by an electrical current, to produce a magnetic field strength of 300 gauss.

The ozonizer incorporates a high-voltage control and regulating circuit (15 kV) that triggers the corona effect, decomposing oxygen into ozone. Oxygen was introduced via an air pump to the ozone generator, which can produce ozone within the range of 0 to 10 g/h. Electrical current was provided by a power source that enables voltage adjustment between 0 and 24 volts, boasting a capacity of 50 A.

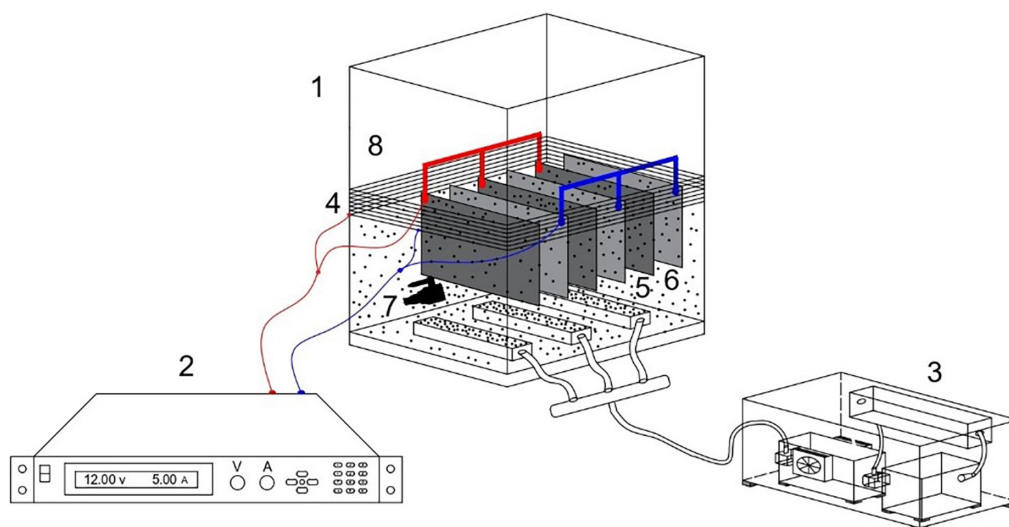


Figure 1. Diagram of the electrocoagulation reactor with serial electrodes: (1) electrocoagulation cell, (2) power source, (3) ozone generator, (4) magnetic-field generator, (5) aluminum cathode, (6) aluminum anode, (7) sampler, and (8) wastewater from tannery

Experimental procedure

In the first stage, preliminary tests were conducted using synthetic and real water to assess the effect of the variables considered in the experimental design. During the preliminary tests, a slight improvement in turbidity and TSS removal was observed when the magnetic field system was coupled with the electrocoagulation reactor. While varying the magnetic field intensity, no significant improvements in turbidity removal were observed. Consequently, a consistent magnetic field strength of 300 gauss was adopted to facilitate the coagulation process. The experimental design was proposed using three current intensity values (3, 5, and 7 A). Under each of these conditions, samples were taken at different times (10, 20, and 30 min), and a specific ozone concentration (4, 7, and 10 g/h) was utilized. To measure pH, conductivity and temperature, an Oakton PCS 35 multiparameter was used. To quantify the COD and TSS, which are considered response variables, a portable DR900 Hach colorimeter was employed. The COD and TSS removal percentages were determined by using Equation (6), as shown below:

$$Y_n = \%R = \left(\frac{C_i - C_f}{C_i} \right) \times 100 \quad (6)$$

where: %R – Removal percentage;
 C_i – Initial Concentration;
 C_f – Final Concentration.

Box-Behnken experimental design

The Response surface method (RSM) is the methodology used for developing optimization models and processes (Ravikumaret al., 2005). The treatment process was optimized based on the Box-Behnken design (BBD), which was developed as a RSM tool to achieve maximum TSS removal using regression coefficient values (R²), adjusted R², and predicted R². As depicted in Equation 7 below, the RSM methodology quantitatively represents independent parameters.

$$y = f(x_1, x_2, x_3, \dots, x_n) \pm \varepsilon \quad (7)$$

where: y – the dependent variable (response parameter);
 f – the response function;
 ε – the experimental error;
 x₁, x₂, x₃, ..., x_n – the independent parameters;

Table 2. Independent variable ranges and their levels

Factor	Variables	Levels		
		-1	0	+1
x ₁	Current intensity (A)	3	5	7
x ₂	Time (min)	10	20	30
x ₃	Ozone (g/h)	4	7	10

To perform the statistical analysis, the Design Expert 11.1 software was used, which reported an ANOVA table at a 95% confidence level. The quality of fit of the polynomial model was expressed by the coefficient of determination R_{2y}R_{adj}. The experimental design was set up with four factors and three levels. The factors considered as independent variables were electric current intensity (x₁), treatment time (x₂), and ozone concentration (x₃). In addition, the percentage of COD (y₁) and TSS (y₂) removal were defined as response variables (Table 2).

RESULTS AND DISCUSSION

Results from the Box-Behnken design

The results of COD and TSS removal expressed as the response variable by EC were sorted according to the design matrix, as shown in Table 3. BBD

Table 3. Quadratic regression model for COD and TSS removal

Exp. No	Factors			Removal COD (%)	Removal TSS (%)
	Current intensity (A)	Treatment time (min)	Ozone (g/h)	Current value	Current value
	x ₁	x ₂	x ₃	y ₁	y ₂
1	3	20	4	29	74
2	7	20	10	35	91
3	3	30	7	35	92
4	5	10	10	9	47
5	5	10	4	15	57
6	5	30	4	37	93
7	5	30	10	36	93
8	7	10	7	14	59
9	7	20	4	36	87
10	7	30	7	39	92
11	3	10	7	4	32
12	3	20	10	15	59
13	5	20	7	29	86
14	5	20	7	30	85
15	5	20	7	28	87

Table 4. ANOVA

	Variation Source	Sum of Squares	DF	MS	F-test	P-value
COD removal (%)	x_1 : Current Intensity (A)	210.13	1	210.13	28.20	0.0032
	x_2 : Time (min)	1378.12	1	1378.12	148.98	< 0.0001
	x_3 : Ozone (g/h)	60.50	1	60.50	8.12	0.0358
	x_1x_2	9.00	1	9.00	1.21	0.3218
	x_1x_3	42.25	1	42.25	5.67	0.0631
	x_2x_3	6.25	1	6.25	0.8389	0.4017
	x_1^2	2.08	1	2.08	0.2788	0.6201
	x_2^2	101.77	1	101.71	13.66	0.0141
	x_3^2	0.9231	1	0.9231	0.1239	0.7392
	Residual	37.25	5	7.45		
	Lack of fit	35.25	3	11.75	11.75	0.0794
	Pure error	2.00	2	1.0000		
	Cor total	1848.93	14			
		$R^2 = 97.99\%$, Adj $R^2 = 94.36\%$				
TSS removal (%)	x_1 : Current intensity (A)	648.00	1	648.00	56.10	0.0007
	x_2 : Time (min)	3828.12	1	3828.12	331.44	< 0.0001
	x_3 : Ozone (g/h)	55.13	1	55.13	4.77	0.0806
	x_1x_2	128.25	1	128.25	15.78	0.0106
	x_1x_3	90.25	1	90.25	7.81	0.0382
	x_2x_3	25.00	1	25.00	2.16	0.2012
	x_1^2	132.92	1	132.92	11.51	0.0194
	x_2^2	467.31	1	467.31	40.46	0.0014
	x_3^2	18.69	1	18.69	1.62	0.2593
	Residual	57.75	5	11.55		
	Lack of fit	55.75	3	18.58	18.58	0.0515
	Pure error	2.00	2	1.0000		
	Cor total	5455.60	14			
		$R^2 = 98.94\%$, Adj $R^2 = 97.04\%$				

included 13 experimental sets and two core experiments. The statistical analysis was performed using Design Expert 11 software. Using multiple regression analysis, the COD (y_1) and TSS (y_2) removal percentage response variables were correlated against the three design factors (x_1, x_2, x_3) using the second-order polynomial (Equation 7). Table 5 lists the quadratic regression model for COD ($y_1\%$) and TSS ($y_2\%$) removal in terms of coded factors.

In addition, an ANOVA yielded a 95% confidence level, comparing the variation sources

against Fisher’s distribution (F-test) to validate the viability of the regression model. In this study, the R^2 value for COD and SST removal with aluminum electrodes is $R^2 = 0.9799$ and $R^2 = 0.9894$ respectively, which demonstrates a good model adequacy, as shown in Tables 4 and 5.

Effect of current intensity

Current intensity is the most important parameter in the electrocoagulation process, as it

Table 5. Statistical parameters obtained by RMS (%)

Answer	R^2	Adj - R^2	p	Quadratic response model based on least squares
	(%)	(%)		
COD removal (%)	97.99	94.36	0.0001	$y_1 = -9.31944 + 2.14583x_1 + 3.49583x_2 - 5.23611x_3 - 0.075x_1x_2 + 0.541667x_1x_3 + 0.041667x_2x_3 - 0.1875x_1^2 - 0.0525x_2^2 + 0.055556x_3^2$
TSS removal (%)	98.94	97.04	0.0001	$y_2 = -63.2500 + 20.70833x_1 + 7.79167x_2 - 3x_3 - 0.3375x_1x_2 + 0.791667x_1x_3 + 0.083333x_2x_3 - 1.5x_1^2 - 0.1125x_2^2 - 0.25x_3^2$

Note: (COD, TSS removal, %); y_1, y_2 (Current intensity, A); x_1 (Time, min); x_2 (Ozone); x_3 .

controls both coagulant dosing and reaction rates within the medium (Nasrullah, 2019). As the current intensity increases, the number of coagulants (anodic aluminum dissolution) and the rate of bubble production rise, leading to an enhanced efficiency of coagulation and flotation of contaminants by the H_2 gas (Kobyas et al., 2006). However, excessively high current intensities applied over extended periods decrease efficiency due to oxygen production and the passivation of aluminum electrodes (Piña et al., 2011). For this study, three current intensity levels (3, 5, and 7 A) were utilized. Figures 2 and 3 illustrate the relationship between COD and TSS removal efficiency and the increase in current intensity. The findings demonstrate that elevating the current intensity from 3 to 7 A results in an efficiency increase of up to 39% for COD removal, while TSS removal reaches a high efficiency of 93%. Here, it is evident that values ≤ 3 A have not exhibited a significant improvement in COD removal efficiency. The achieved COD removal results are comparatively lower than those reported by Barzegar et al. (2018), who documented 85% efficiency with an ozone concentration of 47.4 mg/l, and a current density of 15 mA/cm². In this study, the authors also pointed out the substantial catalytic activity of iron electrodes for ozone activation, in contrast to that of aluminum electrodes. Likewise, Alcocer-Meneses et al. (2022), employing tannery effluents and combining electrocoagulation with ozone, obtained similar values, thereby reporting a 33.2% COD removal efficiency. On a different note, Ahangarnokolaei et al. (2021) reported a 70% COD removal efficiency in a hybrid electrocoagulation-ozone system with aluminum electrodes and 30-min duration. Another study conducted by Wagh and Nemade (2017) reported higher efficiency values with ozone-assisted electrocoagulation, achieving efficiencies of 72% with a current density of 9.75 A cm⁻².

Effect of treatment time

According to Faraday's law, the electrolysis time in the electrocoagulation process affects the release rate of metal ions in the system (Malakootian et al., 2010). The length of electrolysis has a considerable impact on treatment effectiveness in electrochemical processes. The efficiencies of removing COD and TSS were assessed after 10, 20, and 30 min of treatment. Metal ions (acting as coagulants) were generated from anode dissolution

as current passes through the electrode (Bishwama et al., 2022). The concentration of Al^{3+} ions and their hydroxide precipitates increase with extended electrolysis time, resulting in improved TSS removal. In addition, identifying the optimal duration for the electrocoagulation process is crucial to circumvent the needless consumption of resources and energy (Shokri et al., 2022). As shown in Table 3 as well as Figures 2 and 3, the results from this parameter confirm that COD and TSS removal efficiencies increase over the course of the treatment time, particularly after 20 min of treatment. Regarding COD, efficiencies of up to 35% are achieved, while that of TSS removal exceeds 85%. These values differ from those reported by Aboulhassan et al. (2018), who documented 64% efficiency in COD removal. Conversely, the efficiencies of TSS removal are quite similar, reaching a value of 96%. Espinoza et al. (2009) and Varant et al. (2014) also reported high efficiencies, close to 75%, confirming the necessity of utilizing a tertiary system to degrade recalcitrant organic matter. Furthermore, Barzegar et al. (2018) reported efficiencies exceeding 85% with 60-min treatment duration. Nevertheless, in the electrocoagulation process, it is essential to identify the optimal treatment duration, as excessively prolonged periods can lead to elevated electrode and energy consumption (Can et al., 2006).

Effect of ozone concentration

The effect of ozone concentrations on COD and TSS removal was assessed at three levels: 4, 7, and 10 mg/h. The degradation of ozone in water follows a sequential mechanism involving initiation, propagation, and termination stages. Depending on the pH, molecular ozone and hydroxyl radicals generated during this process interact with a range of organic and inorganic compounds present in the effluent, serving as the primary driving force behind the oxidation process. Existing literature provides evidence that in aqueous solutions, the prevailing oxidants are molecular ozone under acidic conditions and hydroxyl radicals under alkaline conditions (Pranjal et al., 2021). During ozonation, the reduction in COD and BOD can be attributed to the oxidation of contaminants by ozone in the water. Ozonation pathways encompass both direct oxidation by ozone and radical oxidation by the OH radicals. Direct oxidation is more selective and prominent under acidic conditions, whereas radical oxidation is less selective

and dominant under alkaline conditions (Pranjal et al., 2021; Mondal et al., 2018). Table 3 reveals that optimal removal efficiencies for COD, 35% and 39%, respectively, were achieved with ozone doses of 7 and 10 g/h. These results contrast with

the findings reported by Ahangarnokolaie et al. (2021), who achieved 51% efficiency with a dose of 1.06 g/h. In addition, Barzegar et al. reported 85% COD removal efficiency in graywater using an ozone dose of 47.4 mg/l and treatment duration

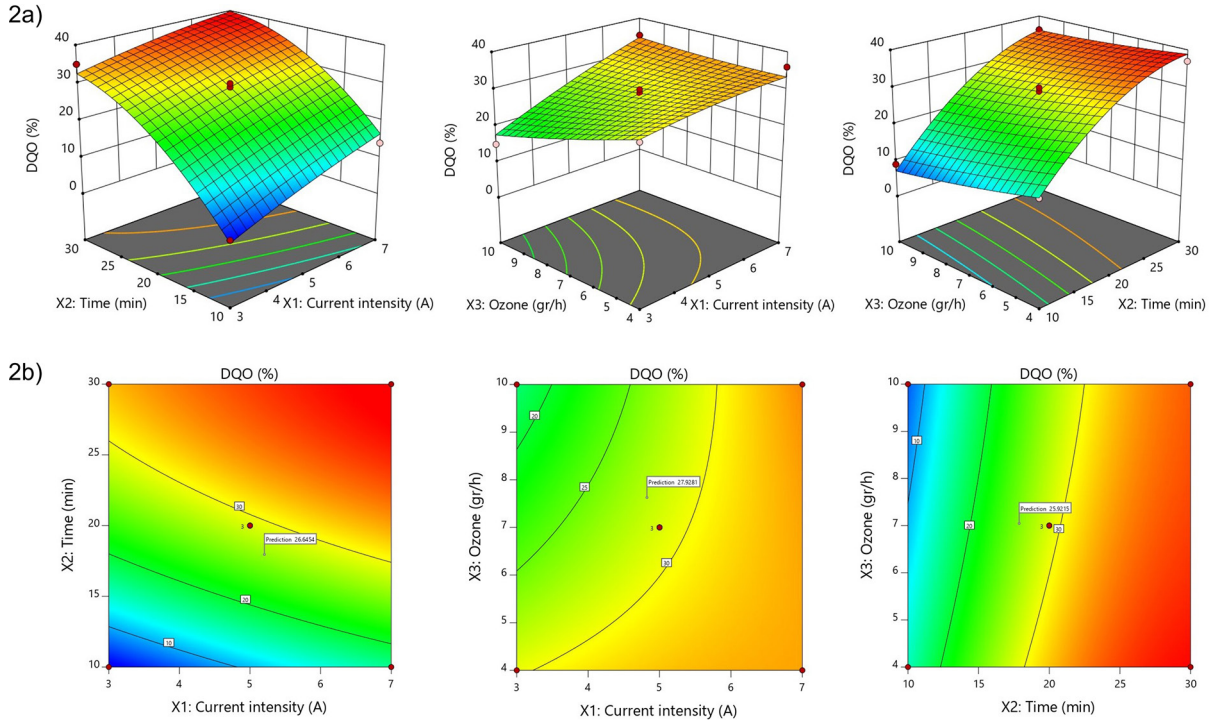


Figure 2. Response surface plot (2a) and contour lines (2b) of the combined effect of current density, treatment time and ozone concentration on COD removal

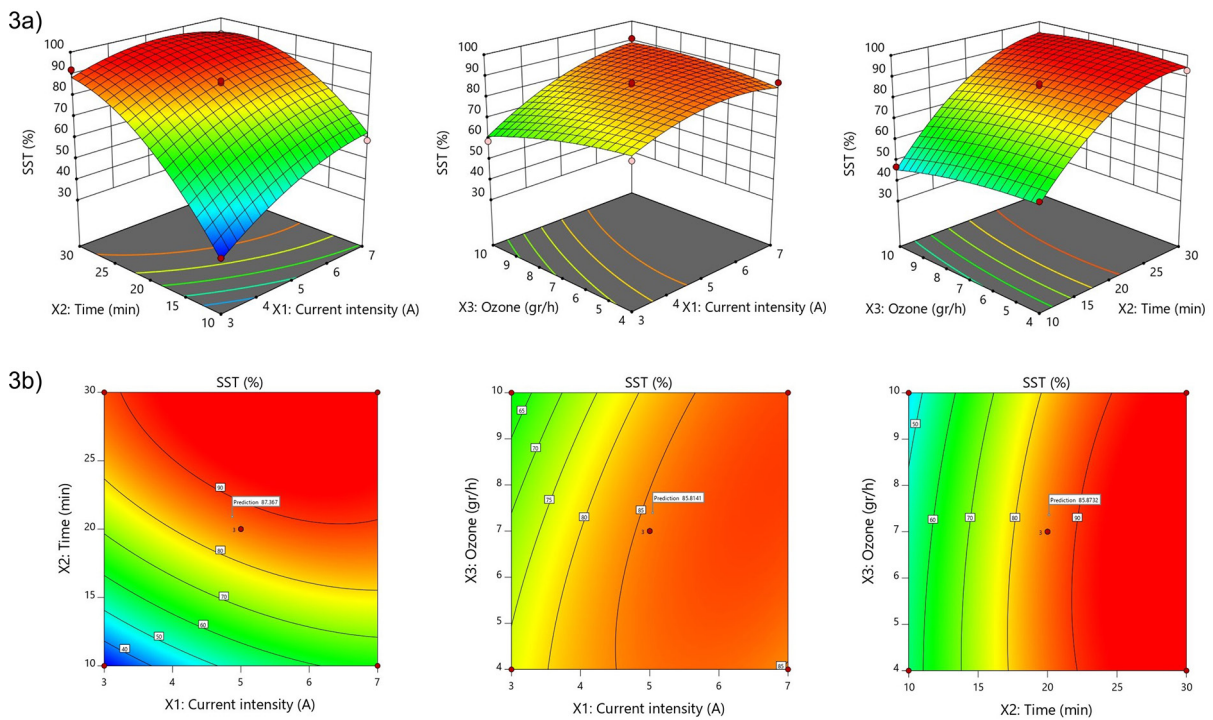


Figure 3. Response surface plot (3a) and contour lines (3b) of the combined effect of current density, treatment time and ozone concentration on TSS removal

of 60 min. Another noteworthy observation is that the concurrent application of EC and ozonation within the same reaction vessel induces increased turbulence in the reactor. This disruption affects the previously stabilized colloidal particles undergoing sedimentation and flotation, thereby reducing the process efficiency.

Optimization of total chromium removal electrocoagulation

The Box-Behnken RSM was utilized for numerical optimization and to establish the optimal parameters that maximize the efficiency of removing COD (y_1) and TSS (y_2). The impact of process variables is illustrated in Figures 2 and 3, which present three-dimensional (3D) and contour (2D) response surface plots. In these graphs, which are based on the mathematical models developed in Equation 7, the variation of the COD and TSS removal percentages can be observed based on their factors of current intensity (x_1), treatment time (x_2) and ozone concentration (x_3). The optimization model predicts that, for COD, the optimal conditions are obtained with values of $I = 6.8$ A, $T = 30$ min, and $O_3 = 10$ mg/l, with an optimum removal of 41.72%. For TSS, an optimal removal of 97% is reached at $I = 5.72$ A, $T = 28$ min and $O_3 = 7.8$.

CONCLUSIONS

The results of this study have demonstrated the efficacy of an integrated system comprising electrocoagulation, magnetic field, and ozonation for the removal of COD and TSS from tannery wastewater. During initial tests, the combination of the magnetic field system and the electrocoagulation reactor did not notably enhance TSS removal as a coagulation aid. However, the results indicate that current intensity, treatment time, and ozone concentration played significant roles in the removal of COD and TSS. The R^2 correlation coefficients for COD and TSS were 97.94% and 98.94%, respectively, indicating a strong model fit. Optimal operating conditions for COD were found to be $I = 6.8$ A, $T = 30$ min, and $O_3 = 10$ mg/l. For TSS, the optimal conditions were $I = 5.72$ A, $T = 28$ min, and $O_3 = 7.8$ mg/l. Consequently, under these conditions, optimal removal rates of 41.8% for COD and 97.9% for TSS were achieved. Furthermore, it can be concluded that

the ozonation system must be used in a separate compartment to prevent the bubbling from ozone diffusers from interfering with the floc formation generated during the electrocoagulation process.

Acknowledgements

The authors thank the Scientific Research Institute of the University of Lima for promoting the integral development of this project and Center for Productive Innovation and Technological Transfer of Leather and Footwear (CITEccal Lima).

REFERENCES

1. Aboulhassan M.A., El Ouarghi H., Ait Benichou S., Ait Boughrou A., Khalil F. 2018. Influence of experimental parameters in the treatment of tannery wastewater by electrocoagulation, *Separation Science and Technology*, 53(17), 2717-2726, DOI: 10.1080/01496395.2018.1470642.
2. Aguilar E., Marrufo L., Neyra W. 2019. Reduction of Total Chromium Levels from Raw Tannery Wastewater via Electrocoagulation using Response Surface Methodology. *Journal of Ecological Engineering. J. Ecol. Eng.* 2019; 20(11), 217–224 <https://doi.org/10.12911/22998993/113191>.
3. Aguilar E., Marrufo L., Neyra W. 2020. Efficiency of electrocoagulation method to reduce COD, BOD and TSS in tannery industry wastewater: application of the box-behnken design. *Leather and Footwear Journal*. <https://doi.org/10.24264/lfj.20.3.1>.
4. Ahangarnokolaei M.A., Ayati B., Ganjidoust H. 2021. Simultaneous and sequential combination of electrocoagulation and ozonation by Al and Fe electrodes for DirectBlue71 treatment in a new reactor: Synergistic effect and kinetics study, *Chemosphere*, 285,131424. <https://doi.org/10.1016/j.chemosphere.2021.131424>.
5. Alcocer-Meneses P., Cabrera-Salazar A.B., Medina-Collana J.T., Rosales-Huamani J.A., Franco-Gonzales E.J., Reyna-Mendoza G.E. 2022. Effects of the Operational Parameters in a Coupled Process of Electrocoagulation and Advanced Oxidation in the Removal of Turbidity in Wastewater from a Curtember. *Appl. Sci.* 12, 8158. <https://doi.org/10.3390/app12168158>.
6. Asaithambi P., Aziz A.R.A., Daud W.M.A.B.W. 2016. Integrated ozone—electrocoagulation process for the removal of pollutant from industrial effluent: optimization through response surface methodology. *Chem. Eng. Process*, 105, 92–102. <https://doi.org/10.1016/j.cep.2016.03.013>.
7. Barzegar Gelavizh., Wu Junxue., Ghanbari Farshid. 2019. Enhanced treatment of greywater

- using electrocoagulation/ozonation: Investigation of process parameters. *Process Safety and Environmental Protection*, 121. 10.1016/j.psep.2018.10.013.
8. Bilińska L., Blus k., Gmurek M., Ledakowicz S. 2019. Coupling of electrocoagulation and ozone treatment for textile wastewater reuse, *Chem. Eng. J.* 358(2019), 992–1001. <https://doi.org/10.1016/j.cej.2018.10.093>.
 9. Bishwatma Biswas., Sudha Goel. 2022. Electrocoagulation and electrooxidation technologies for pesticide removal from water or wastewater: A review, *Chemosphere*, Volume 302, 134709. <https://doi.org/10.1016/j.chemosphere.2022.134709>.
 10. Can O.T., Kobya M., Demirbas E., Bayramoglu M. 2006. Treatment of the textile wastewater by combined electrocoagulation. *Chemosphere* 62, 181e187. <https://doi.org/10.1016/j.chemosphere.2005.05.022>.
 11. Cho Y.I., Lee S.H. 2005. Reduction in the surface tension of water due to physical water treatment for fouling control in heat exchangers. *International Communications in Heat and Mass Transfer*, 3(1–2), 1–9. doi: 10.1016/j.icheatmasstransfer.2004.03.019.
 12. De la Luz-Pedro A., Efraín F., Martínez P., López-Araiza M.H., Jaime-Ferrer S., Estrada-Monje A., Bañuelos A. 2019. “Pollutant Removal from Wastewater at Different Stages of the Tanning Process by Electrocoagulation”, *Journal of Chemistry*, vol. 2019, Article ID 8162931, 9 pages, 2019. <https://doi.org/10.1155/2019/8162931>.
 13. Dermentzis K.I. 2016. Removal of sulfide and COD from a crude oil wastewater model by aluminum and iron electrocoagulation. *J. Eng. Sci. Technol. Rev.* 9, 13–16.
 14. Ebba Million. 2021. Studies on electrode combination for COD removal from domestic wastewater using electrocoagulation. *Heliyon*. 7. <https://doi.org/10.1016/j.heliyon.2021.e08614>.
 15. Esfandyari Y., Saeb K., Tavana A., Rahnavard A., Fahimi F.G. 2019. Effective removal of cefazolin from hospital wastewater by the electrocoagulation process. *Water Sci. Technol.* 80, 2422–2429.
 16. Espinoza-Quñones F.R., Fornari M.M.T., Modenes A.N., Palacio S.M., Trigueros D.E.G., Borba F.H., Kroumov A.D. 2009. Electrocoagulation efficiency of the tannery effluent treatment using aluminum electrodes, *Water Sci Technol*, 2009, 60, 2173–2185. <https://doi.org/10.2166/wst.2009.518>.
 17. Garcés-Pineda F.A., Blasco-Ahicart M., Nieto-Castro D., López N., Galán-Mascarós J.R. 2019. Direct magnetic enhancement of electrocatalytic water oxidation in alkaline media. *Nature Energy*, 4, 519–425.
 18. Ghernaout D., Ghernaout B., Saiba A., Boucherit A., Kellil A. 2009. Removal of humic acids by continuous electromagnetic treatment followed by electrocoagulation in batch using aluminium electrodes, *Desalination*, 239(1–3), 295–308. <https://doi.org/10.1016/j.desal.2008.04.001>
 19. Guo Z., Jian Guo Cui J., Gang Wei. 2014. The Effect of Applied Magnetic Field on the Mine Water Coagulation Applied Mechanics and Materials (Volumes 522–524) 1021–1026. <https://doi.org/10.4028/www.scientific.net/AMM.522-524.1021>.
 20. Hernández-Ortega M., Ponziak T., Barrera-Díaz C., Rodrigo M.A., Roa-Morales G., Bilyeu B. 2010. Use of a combined electrocoagulation–ozone process as a pretreatment for industrial wastewater. *Desalination* 250, 144–149. <https://doi.org/10.1016/j.desal.2008.11.021>.
 21. Holt P., Barton G., Mitchell C. 2005. The future for electrocoagulation as a localized water treatment technology. *Chemosphere*, 59, 355–367. <http://dx.doi.org/10.1016/j.chemosphere.2004.10.023>.
 22. Ibanez J.G., Vazquez-Olavarieta J.L., Hernandez-Rivera L., Garcia-Sanchez M.A., Garcia-Pintor E. 2012. A novel combined electrochemical-magnetic method for water treatment. *Water Sci. Technol.* 65, 2079. <https://doi.org/10.2166/wst.2012.108>.
 23. Irki Sara & Ghernaout Djamel, Naceur Wahib. 2017. Decolourization of Methyl Orange (MO) by Electrocoagulation (EC) using Iron Electrodes under a Magnetic Field (MF). *Desalination and water treatment*. 79. 368–377. 10.5004/dwt.2017.20797.
 24. Johan S., Fadil O., Zularisham A. 2004. Effect of magnetic fields on suspended particles in Sewage. *Malaysian Journal of Science*, 23, 141–148. <https://doi.org/10.12962/j25983806.v5.i3.317>.
 25. Joseph C.G., Farm Y.Y., Taufiq-Yap Y.H., Pang C.K., Nga J.L., Puma G.L. 2021. Ozonation treatment processes for the remediation of detergent wastewater: a comprehensive review. *J. Environ. Chem. Eng.* 106099. <https://doi.org/10.1016/j.jece.2021.106099>.
 26. Kanagaraj J., Senthivelan T., Panda R.C., Kavitha S. 2014. Eco-friendly waste management strategies for greener environment towards sustainable development in leather industry: A comprehensive review. *Journal of Cleaner Production*. <https://doi.org/10.1016/j.jclepro.2014.11.013>.
 27. Kobya M., Demirbas E., Can OT., Bayramoglu M. 2006. Treatment of levafix orange textile dye solution by electrocoagulation, *J. Hazard. Mater.* 132 (2006) 183–188. <https://doi.org/10.1016/j.jhazmat.2005.07.084>.
 28. Koyuncu S., Arıman S. 2020. Domestic wastewater treatment by real-scale electrocoagulation process. *Water Sci. Technol.* 1–12.
 29. Liu Y., Yang J., Jiang W., Chen Y., Yang Ch., Wang T., Li Y. 2018. Experimental studies on the enhanced performance of lightweight oil recovery using a combined electrocoagulation and magnetic field processes. *Chemosphere* 205, 601–609. <https://doi.org/10.1016/j.chemosphere.2018.04.113>.

30. Liu Z., Demeestere K., Hulle S.V. 2021. Comparison and performance assessment of ozone-based AOPs in view of trace organic contaminants abatement in water and wastewater: a review, *J. Environ. Chem. Eng.* 9 (2021) 105–599. <https://doi.org/10.1016/j.jece.2021.105599>.
31. Malakootian M., Mansoorian H.J., Moosazadeh M. 2010. Performance evaluation of electrocoagulation process using iron-rod electrodes for removing hardness from drinking water, *Desalination*, Volume 255, Issues 1–3, 2010, Pages 67–71. <https://doi.org/10.1016/j.desal.2010.01.015>.
32. Malik S.N., Ghosh A.N., Vaidya A.N., Mudliar S.N. 2020. Hybrid ozonation process for industrial wastewater treatment: principles and applications: a review, *J. Water Process Eng.* 35 (2020), 101193. <https://doi.org/10.1016/j.jwpe.2020.101193>
33. Mondal S., Purkait M. K., De S. 2018. Adsorption of dyes. In *Advances in Dye Removal Technologies*, pp. 49–98. Springer, Singapore. https://doi.org/10.1007/978-981-10-6293-3_2.
34. Moussa D.T., El-Naas M.H., Nasser M., Al-Marri M.J. 2017. A comprehensive review of electrocoagulation for water treatment: potentials and challenges. *J. Environ. Manag.* 186, 24–41. <https://doi.org/10.1016/j.jenvman.2016.10.032>.
35. Nasrullah M., Zularisam A.W., Krishnan S., Sakinah M., Singh L., Fen Y.W. 2019. High performance electrocoagulation process in treating palm oil mill effluent using high current intensity application. *Chin. J. Chem. Eng.* 27, 208–217. <http://dx.doi.org/10.1016/j.cjche.2018.07.021>.
36. Nugroho F., Aryanti P., Nurhayati S., Muna H. 2019. A combined electrocoagulation and mixing process for contaminated river water treatment, *AIP Conf Proc.* AIP Publishing LLC, pp.030017. <https://doi.org/10.1063/1.5098192>.
37. Papadopoulos K.P., Argyriou R., Economou C.N., Charalampous N., Dailianis S., Tatoulis T.I., Tekerekopoulou A.G., Vayenas D.V. 2019. Treatment of printing ink wastewater using electrocoagulation. *J. Environ. Manag.* 237, 442–448. <https://doi.org/10.1016/j.jenvman.2019.02.080>.
38. Piña M., Martín A., González C., Prieto F., Guevara A., García J. 2011. Revisión de variables de diseño y condiciones de operación en la electrocoagulación. *Revista Mexicana de Ingeniería Química*, 10(2),257-271. Recuperado de http://www.scielo.org.mx/scielo.php?script=sci_rtext&pid=S1665-27382011000200010.
39. Pranjali P. Das et al. 2021. "Integrated ozonation assisted electrocoagulation process for the removal of cyanide from steel industry wastewater," *Chemosphere*, 263, 128370.
40. Ravikumar K., Deebika B., Balu K. 2005. Decolorization of aqueous dye solutions by a novel adsorbent: application of statistical designs and surface plots for the optimization and regression analysis *J. Hazard. Mater.*, 22 (2005), 75–83.
41. Shokri A., Fard M.S. 2022. A critical review in electrocoagulation technology applied for oil removal in industrial wastewater. *Chemosphere*, 288, 132355. <https://doi.org/10.1016/j.chemosphere.2021.132355>.
42. Wagh M.P., Nemade P.D. 2017. An influence of experimental parameters in the treatment of anaerobically treated distillery spent wash by using ozone assisted electrocoagulation *83(2017)*, 7–15. <https://doi.org/10.5004/dwt.2017.21041>.
43. Yasri Nael., Nightingal Michael Nightingal., Keith J. Cleland., Edward P.L. Roberts. 2022. The impact of a magnetic field on electrode fouling during electrocoagulation, *Chemosphere*, 2022, 135207, <https://doi.org/10.1016/j.chemosphere.2022.135207>.
44. Varank G., Erkan H., Yazıcı S., Demir A., Engin G. 2014. Electrocoagulation of tannery wastewater using monopolar electrodes: process optimization by response surface methodology, *Int J Environ Res*, 2014, 8, 165–180. <http://dx.doi.org/10.22059/IJER.2014.706>.